Description of the simplest photonuclear reactions within the particle-hole dispersive optical model

B. A. Tulupov
Institute for Nuclear Research RAS, 117312 Moscow, Russia

M. H. Urin
National Research Nuclear University "MEPhI" (Moscow Engineering Physics Institute), 115409 Moscow, Russia

(Received 26 June 2014; published 18 September 2014)

A recently developed particle-hole dispersive optical model is applied to describe the cross sections of photoabsorption, direct + semidirect photoneutron and inverse reactions accompanied by excitation of the isovector giant dipole and quadrupole resonances in medium–heavy-mass spherical nuclei. The model is an extension of the standard and nonstandard versions of the continuum-random-phase approximation by including the spreading effect in a phenomenological way. It contains the following ingredients: the Landau–Migdal particle-hole interaction and a phenomenological mean field consistent with this interaction, isovector velocity-dependent forces taken in the simplest form and the imaginary part of an effective single-particle optical-model potential determining the corresponding dispersive part. All the model parameters are taken from the other data and from the description of photoabsorption, while the direct + semidirect photoneutron and inverse reactions are described without the use of specific adjustable parameters. Calculation results obtained for a few neutron-closed-shell nuclei are compared with the corresponding experimental data.

DOI: 10.1103/PhysRevC.90.034613 PACS number(s): 21.60.Jz, 24.10.Ht, 24.30.Cz, 25.20.−x

I. INTRODUCTION

The isovector giant dipole resonance (IVGDR) predicted by Migdal [1] and soon after observed experimentally [2] was intensively studied together with the isovector giant quadrupole resonance (IVGQR) by means of the simplest photonuclear reactions. These are photoabsorption, direct + semidirect (DSD) photonucleon, and inverse reactions (see, e.g., Ref. [3]). The photoabsorption cross section, which is mainly proportional to the IVGDR strength function, was described within quite a few semiclassical and microscopic approaches. The DSD photonucleon and inverse reactions accompanied by IVGDR excitation in medium–heavy-mass nuclei were described, during the last decades, only within the so-called DSD model proposed by Brown [4] and extended by the Ljubljana group (see, e.g., Ref. [5] and references therein). The excitation of the IVGQR was also included in the DSD model [6]. Within this model a number of phenomenological quantities are used. One of them, the imaginary part of the IVGDR form factor (transition potential), has no clear physical meaning. Also the calculated DSD-reaction cross sections depend markedly on the choice of the single-particle (s-p) optical model used for evaluation of the escaped (captured) nucleon wave function.

As a phenomenon, the DSD reactions induced by an external s-p field are closely related to direct nucleon decay of high-energy particle–hole-type nuclear excitations, including giant resonances. Therefore, the most adequate description of the DSD reactions seems to be possible within a semimicroscopic model, which provides a good description of the main relaxation modes of the mentioned excitations. For medium–heavy-mass "hard" spherical nuclei (in particular, for singly- and doubly-closed-shell nuclei) these modes are the following: Landau damping and coupling of particle–hole-type states to the s-p continuum and to many-quasiparticle configurations (the spreading effect). Within the recently developed particle-hole (p-h) dispersive optical model (PHDOM) [7,8], Landau damping and coupling to the s-p continuum are considered microscopically, starting from the standard and nonstandard versions of the continuum-random-phase approximation (cRPA), while the spreading effect is described in a phenomenological way in terms of the energy-dependent imaginary part of the effective s-p optical-model potential used in the PHDOM equations. The properly parametrized imaginary part determines also the real potential added to the nuclear mean field via the corresponding dispersive relationship. The model is valid at arbitrary (but high enough) excitation energies.

In this work we present a detailed application of the PHDOM to a description of the simplest photonuclear reactions accompanied by excitation of the IVGDR and IVGQR in a few neutron-closed-shell nuclei. The work is a direct continuation of our previous study of Ref. [9], where the semimicroscopic approach [7,10], corresponding to the PHDOM "pole" version (valid in a vicinity of the given giant resonance), has been exploited. For both approaches the input quantities (Landau–Migdal p-h interaction consistent with the adopted phenomenological mean field, isovector velocity-dependent forces, and an imaginary part of the effective optical-model potential) are the same. The unique feature of the PHDOM and its "pole" version is the description of the DSD reactions without the use of specific adjustable parameters. All the model parameters are taken from the independent data and from the description of the giant resonance strength function. Some results concerned with the applications of the PHDOM to the description of the fast-neutron radiative capture are briefly discussed in Ref. [11]. In the present work we use a somewhat different mean field than that assumed in Ref. [11] to better describe the integrated photoabsorption cross section.

The paper is organized as follows: In Sec. II the PHDOM relationships for the energy-averaged dipole and quadrupole strength functions, DSD $E1$- and $E2$-reaction amplitudes are given together with the description of input quantities and the choice of model parameters. The expressions for observable quantities, calculation results in comparison with the corresponding experimental data, and discussions of the results are presented in Sec. III. Conclusive remarks are given in Sec. IV.

II. BASIC RELATIONSHIPS

A. Equations of the standard and nonstandard versions of cRPA

We start the description of PHDOM basic relationships from the corresponding equations of the standard and nonstandard versions of the cRPA. These equations can be formulated in terms of the effective energy-dependent fields related to the corresponding s-p external fields (see, e.g., Refs. [7,8]). When applied to the description of p-h excitations in the neutral channel, the system of the integral equations for the neutron (n) and proton (p) effective fields can be schematically written in the form

$$V^{\alpha} = V_0^{\alpha} + \sum_{\beta} F^{\alpha\beta} A^{\beta} V^{\beta}. \tag{1}$$

Here, $\alpha(\beta) = n, p$ are the isobaric indexes relating to both the external and effective fields V_0^{α} and $V^{\beta}(\omega)$, respectively, $F^{\alpha\beta}$ is the interaction in the p-h channel, $A^{\beta}(\omega)$ is the free p-h propagator for the subsystem β, and ω is the excitation energy. The effective fields determine the corresponding strength function as follows:

$$S_{V_0} = -\frac{1}{\pi}\mathrm{Im}\sum_{\alpha}\left(V_0^{\alpha}\right)^{*} A^{\alpha} V^{\alpha}. \tag{2}$$

Equations (1) and (2) correspond to the standard cRPA version, which can be also formulated in terms of the effective p-h propagator (see, e.g., Refs. [7,8]). The nonstandard cRPA version is formulated with the use of the effective-field method and based on the alternative representation of the strength function of Eq. (2). This representation follows from Eqs. (1) and (2) and in the continuum region ($\omega > B_N, B_N$ is the nucleon separation energy) can be presented in the following form [7,8]:

$$S_{V_0} = \sum_{\alpha,c}\left|M^{\alpha}_{V_0,c}\right|^2. \tag{3}$$

Being a proper matrix element of the effective field V^{α}, the quantity $M^{\alpha}_{V_0,c}$ is the amplitude of the DSD reaction induced by the external field V_0 (c is a set of the reaction-channel quantum numbers). Actually, Eq. (3) represents a kind of the optical theorem.

Bearing in mind excitations of the IVGDR and IVGQR in photonuclear reactions [generally the isovector dipole ($L = 1$) and isovector + isoscalar quadrupole ($L = 2$) (p-h)-type excitations in the neutral channel], we simplify the isobaric structure of the corresponding external and effective fields [$1 \ll (N - Z) \ll A$]: $V^p_{0,1} = -V^n_{0,1} = (1/2)Q_{1M}$, $V^p_{0,2} = Q_{2M}$, $V^n_{0,2} = 0$, where $Q_{LM} = r^L Y_{LM}$ is the multipole operator. To define the model parameters we use $Q_{00} = r^2 Y_{00}$ as the external field for description of the isoscalar giant monopole resonance excitation. Using these definitions and also the substitution $A^{\alpha} \to A = \frac{1}{2}(A^n + A^p)$, one gets from Eq. (1) two uncoupled equations for the effective fields $V_L^{(\mp)} = V_L^p \mp V_L^n$:

$$V_L^{(\mp)} = V_{0,L}^{(\mp)} + F^{(\mp)} A V_L^{(\mp)}. \tag{4}$$

Here $V^{(-)}_{0,1} = Q_{1M}, V^{(+)}_{0,1} = 0$, $V^{(\mp)}_{0,2} = Q_{2M}$ and $F^{(\mp)} = \frac{1}{2}(F^{pp} \mp F^{pn})$ ($F^{pp} = F^{nn}$, $F^{np} = F^{pn}$). The signs $(-)$ and $(+)$ in Eq. (4) and in the following equations for the strength functions:

$$S_L^{(\mp)} = -\frac{1}{2\pi}\mathrm{Im}((V_{0,L}^{(\mp)})^{*} A V_L^{(\mp)}), \tag{5}$$

are related to the isovector and isoscalar excitations, respectively. It is noteworthy that the neutron effective fields $V_1^n = -\frac{1}{2}V_1^{(-)}$ and $V_2^n = \frac{1}{2}(V_2^{(+)} - V_2^{(-)})$ determine, respectively, the $E1$- and $E2$-photoneutron DSD-reaction amplitudes $M^n_{L,c}$ of Eq. (3). The $E2$ amplitude exists only due to the p-h interaction.

In the following implementations of the PHDOM we use the spinless part of the Landau–Migdal p-h interaction, $[F(r) + F'\boldsymbol{\tau}\boldsymbol{\tau}']\delta(\mathbf{r} - \mathbf{r}')$, and isovector velocity-dependent forces. The necessity to include a momentum-dependent p-h interaction in the description of IVGDR properties was noted in Ref. [12]. Taking this interaction as a sum of separable terms allows us to get the corresponding cRPA equations in a closed form [13]. The expressions for the p-h interaction in the isoscalar ($L = 2$) and isovector ($L = 1,2$) channels with multipolarity L equal 1 or 2 can be presented as follows:

$$F_L^{(+)} = F(r)\frac{\delta(r - r')}{rr'}\sum_M (-1)^M Y_{L-M} Y_{LM},$$

$$F_L^{(-)} = F'\frac{\delta(r - r')}{rr'}\sum_M (-1)^M Y_{L-M} Y_{LM}$$

$$+ \frac{4\pi m k'_L}{(2L+1)AR^{2(L-1)}}\sum_M (-1)^M \dot{Q}_{L-M}\dot{Q}_{LM}. \tag{6}$$

Here, m is the nucleon mass, A is the number of nucleons, R is the nuclear radius, k'_L are the dimensionless intensities of the isovector velocity-dependent forces; $\dot{Q}_{LM} = (i/\hbar)[H_0, Q_{LM}]$, where H_0 is the s-p Hamiltonian. [For the choice of the intensities $F(r) = Cf(r)$, $F' = Cf'$ ($C = 300$ MeV fm^3) and the nuclear mean field see Sec. II C.]

Assuming that the external and corresponding effective fields have the same angular symmetry and taking into account the choice of the p-h interaction according to Eq. (6), we seek the solutions to Eqs. (4) in the form

$$V^{(+)}_{LM}(\mathbf{r},\omega) = V^{(+)}(r,\omega)Y_{LM}(\mathbf{r}/\mathrm{r}) \quad (L = 2), \tag{7}$$

$$V^{(-)}_{L}(\mathbf{r},\omega) = \tilde{V}_L(r,\omega)Y_{LM}(\mathbf{r}/\mathrm{r}) + \Delta_L(\omega)\dot{Q}_{LM}(\mathbf{r}) \quad (L = 1,2). \tag{8}$$

After separation of the spin-angular variables we get from Eqs. (4) the following integral equations for the radial parts of

the isoscalar and isovector effective fields:

$$V_2^{(+)}(r,\omega) = r^2 + \frac{2F(r)}{r^2}\int \mathcal{A}_L(r,r_1;\omega)V_2^{(+)}(r_1,\omega)dr_1, \quad (9)$$

$$V_L^{(-)}(r,\omega) = \tilde{V}_L(r,\omega) + \tilde{V}'_L(r,\omega), \quad (10)$$

$$\tilde{V}_L(r,\omega) = r^L + \frac{2F'}{r^2}\int [\mathcal{A}_L(r,r_1;\omega) + \mathcal{A}'_L(r,r_1;\omega)] \times \tilde{V}_L(r_1,\omega)dr_1, \quad (11)$$

where

$$\mathcal{A}'_L(r,r_1;\omega) = \tilde{k}'_L\omega^2\mathcal{B}_L^{-1}(\omega)\int \mathcal{A}_L(r,r_2;\omega)r_2^L dr_2 \times \int r_3^L\mathcal{A}_L(r_3,r_1;\omega)dr_3, \quad (12)$$

and

$$\tilde{V}'_L(r,\omega) = \tilde{k}'_L\omega^2\mathcal{B}_L^{-1}(\omega)r^L\int r_1^L\mathcal{A}_L(r_1,r_2;\omega)\tilde{V}_L(r_2,\omega)dr_1dr_2. \quad (13)$$

Here, $(rr_1)^{-2}\mathcal{A}_L(r,r_1,\omega)$ is the radial part of the free p-h propagator, corresponding to the excitations with angular momentum L (see, e.g., Ref. [7]),

$$\mathcal{B}_L(\omega) = 1 + \left(\frac{2\overline{r^2}}{R^2}\right)^{(L-1)}k'_L - \omega^2\tilde{k}'_L\int r_1^L\mathcal{A}_L(r_1,r_2;\omega) \times r_2^L dr_1dr_2,$$

where $\overline{r^2}$ is the mean-squared radius and $\tilde{k}'_L = 8\pi mk'_L/[(2L+1)\hbar^2AR^{2(L-1)}]$.

The effective fields found from Eqs. (9)–(13) determine the corresponding strength functions and photoneutron DSD-reaction amplitudes in accordance with the relationships (5) and (3), respectively:

$$S_L^{(\mp)}(\omega) = -\frac{1}{2\pi}\mathrm{Im}\int r^L\mathcal{A}_L(r,r';\omega)V_L^{(\mp)}(r',\omega)drdr' \quad (L=1,2), \quad (14)$$

and

$$M_{1,c}^{(n)}(\omega) = -\frac{1}{2}\left(n_\mu^{(n)}\right)^{1/2}t_{(\lambda)(\mu)}^{(1)}\int \chi^{(+)(n)}_{\varepsilon=\varepsilon_\mu+\omega,(\lambda)}(r)V_1^{(-)}(r,\omega) \times\chi_\mu^{(n)}(r)dr, \quad (15)$$

$$M_{2,c}^{(n)}(\omega) = \frac{1}{2}\left(n_\mu^{(n)}\right)^{1/2}t_{(\lambda)(\mu)}^{(2)}\int \chi^{(+)(n)}_{\varepsilon=\varepsilon_\mu+\omega,(\lambda)}(r)(V_2^{(+)}(r,\omega) - V_2^{(-)}(r,\omega))\chi_\mu^{(n)}(r)dr. \quad (16)$$

Here, $r^{-1}\chi^{(+)(n)}_{\varepsilon,(\lambda)}(r)$ is the single-neutron continuum-state radial wave function normalized to the δ function of the energy ε, $r^{-1}\chi_\mu^{(n)}(r)$ is the single-neutron bound-state radial wave function, $(\lambda) = j_\lambda, l_\lambda$ are the quantum numbers of the s-p total and orbital angular momenta, $n_\mu = N_\mu/(2j_\mu+1)$ is the occupation factor (N_μ is the number of neutrons filling the s-p level μ), and $\sqrt{2L+1}t^{(L)}_{(\lambda)(\mu)} = \langle(\lambda)||Y_L||(\mu)\rangle$ is the reduced matrix element. The set $\mu,(\lambda) = c$ together with the L value are the quantum numbers of the (γ,n)-reaction channel.

B. PHDOM equations

Within the cRPA, only Landau damping of p-h-type states and coupling of these states to the s-p continuum are taken into account. As mentioned in the introduction, the PHDOM is an extension of the cRPA versions by accounting for the spreading effect. Within this model, Landau damping of (p-h)-type states and coupling of these states to the s-p continuum are described microscopically, while the coupling of (p-h)-type states to many-quasiparticle configurations (chaotic states) is treated phenomenologically on average over the energy with the use of a statistical assumption. The latter means that, after energy averaging, the different p-h states having the same angular momentum and parity decay into chaotic states independently of one another. This assumption is exploited in transformation of the energy-averaged equation for the nonlocal p-h Green function (effective p-h propagator) to the equation for the energy-averaged local p-h effective propagator [7,8]. Formally, the result looks like the corresponding cRPA equations, in which the "free" energy-averaged p-h propagator $\mathcal{A}_L^\alpha(r,r',\omega)$ is used. Hereafter, for the ω-dependent energy-averaged quantities we use the same notations as those used for the corresponding cRPA quantities in the previous section. The PHDOM being a basic quantity, this propagator enters in Eqs. (10)–(13) for the energy-averaged effective fields and in Eqs. (14) for the energy-averaged strength functions. Starting from a rather general consideration of Refs. [7,8], we give below the explicit expression for the "free" energy-averaged p-h propagator in the form, which is further directly used in calculations:

$$\mathcal{A}_L = \mathcal{A}_L^{(1)} + \mathcal{A}_L^{(2)} + \mathcal{A}_L^{(3)},$$

$$\mathcal{A}_L^{(1)} = \sum_{\mu,(\lambda)} n_\mu\left(t^L_{(\lambda)(\mu)}\right)^2\chi_\mu(r)\chi_\mu(r')g_{(\lambda)}(r,r',\varepsilon_\mu+\omega),$$

$$\mathcal{A}_L^{(2)} = \sum_{\lambda,(\mu)} n_\lambda\left(t^L_{(\mu)(\lambda)}\right)^2\chi_\lambda(r)\chi_\lambda(r')g_{(\mu)}(r',r,\varepsilon_\mu-\omega),$$

$$\mathcal{A}_L^{(3)} = 2\sum_{\mu,\lambda} n_\mu n_\lambda\left(t^L_{(\mu)(\lambda)}\right)^2\chi_\mu(r)\chi_\mu(r')\chi_\lambda(r)\chi_\lambda(r') \times \frac{[iW(\omega)-P(\omega)]f_\mu f_\lambda}{(\varepsilon_\lambda-\varepsilon_\mu+\omega)^2 - [iW(\omega)-P(\omega)]^2f_\mu^2f_\lambda^2}. \quad (17)$$

For brevity, the isobaric index was omitted. In Eq. (17), $(rr')^{-1}g_{(\lambda)}(r,r',\varepsilon)$ and $(rr')^{-1}g_{(\mu)}(r',r,\varepsilon)$ are the optical-model radial Green functions satisfying the equations

$$-\delta(r-r') = (h_{0,(\lambda)}(r) - \{\varepsilon_\mu+\omega+[iW(\omega)-P(\omega)] \times f_\mu f_{\mathrm{WS}}(r)\})g_{(\lambda)}(r,r',\varepsilon_\mu+\omega), \quad (18)$$

$$-\delta(r'-r) = (h_{0,(\mu)}(r') - \{\varepsilon_\lambda-\omega+[iW(\omega)-P(\omega)] \times f_\lambda f_{\mathrm{WS}}(r')\})g_{(\mu)}(r',r,\varepsilon_\lambda-\omega), \quad (19)$$

with $h_{0,(\lambda)}(r)$ and $[-iW(\omega)+P(\omega)]f_\mu f_{\mathrm{WS}}(r)$ being, respectively, the radial part of a s-p Hamiltonian (including the spin-orbit and centrifugal terms) and the optical-model

addition to the nuclear mean field, [$f_{\rm WS}(r)$ is the Woods–Saxon function and $f_\mu = \int f_{\rm WS}(r)\chi^2_\mu(r)dr$]. The intensity of the imaginary part of the effective optical-model potential, $W(\omega)$, is considered as a phenomenological quantity, while the real part $P(\omega)$ appearing due to a spreading effect is determined by $W(\omega)$ via a proper dispersive relationship [7,8,14].

Extension of the nonstandard cRPA version consists of taking into account the spreading effect on the DSD-reaction amplitudes of Eqs. (15) and (16). Within the PHDOM, the energy-averaged amplitudes are expressed via energy-averaged effective fields and also via the optical-model continuum-state wave function $\chi^{(+)}_{\varepsilon=\varepsilon_\mu+\omega,(\lambda)}(r,\omega)$, satisfying the homogeneous equation (18) [8].

The above-described energy-averaged strength functions and DSD-reaction amplitudes are further used for the evaluation of the energy-averaged photoabsorption, DSD photoneutron, and inverse-reaction cross sections.

C. Input quantities: Choice of model parameters

As mentioned in the introduction, the p-h interaction, a phenomenological mean field partially consistent with this interaction, and the imaginary part of the effective optical-model potential are the input quantities for implementations of the PHDOM. The p-h interaction used for description of the simplest photonuclear reactions is presented in Sec. II A. The phenomenological mean field $U^\alpha_\lambda(r)$, which enters in the Schrödinger equations for radial Green and wave functions, contains the isoscalar (central and spin orbit), the isovector, and the Coulomb parts ($\tau^n = 1$, $\tau^p = -1$):

$$U^\alpha_{(\lambda)}(r) = U_0(r) + U_{ls,(\lambda)}(r) + \tfrac{1}{2}v(r)\tau^\alpha + \tfrac{1}{2}(1-\tau^\alpha)U_C(r). \tag{20}$$

Here, the isoscalar terms

$$U_0(r) = -U_0 f_{\rm WS}(r,R,a),$$
$$U_{ls,(\lambda)}(r) = U_{ls}\frac{1}{r}\frac{df_{\rm WS}}{dr}(\mathbf{ls})_{(\lambda)}, \tag{21}$$

where $f_{\rm WS}(r,R,a) = [1+\exp(\frac{r-R}{a})]^{-1}$ are considered as purely phenomenological quantities, while the isovector and Coulomb parts

$$v(r) = 2f'n^{(-)}(r), \quad U_C(n^{(p)}) \tag{22}$$

are calculated self-consistently via the neutron excess and proton densities, respectively. The above-described mean field is determined by five adjustable parameters U_0, U_{ls}, $r_0 = RA^{-1/3}$, a, and f'. They are chosen from a fit to the observed single-quasiparticle spectra in doubly-closed-shell nuclei ^{48}Ca, ^{132}Sn, and ^{208}Pb, carried out in Refs. [15,16]. For other nuclei these parameters are obtained by an interpolation procedure. Determined in this way, the above-mentioned parameters for ^{89}Y, ^{140}Ce, and ^{208}Pb are listed in Table I.

Turning to the p-h interaction of Eq. (6), we note the following: The dimensionless intensity of the isoscalar part of the Landau–Migdal interaction is parametrized in accordance with Ref. [12]: $f(r) = f^{ex} + (f^{in} - f^{ex})f_{\rm WS}(r)$. The main parameter f^{ex} is found from the condition that the isoscalar 1^- spurious state, related to center-of-mass motion, lies at zero energy. For this purpose the strength function $S^{(+)}_1(\omega)$ of Eq. (14), corresponding to the isoscalar external field $V^{(+)}_{0,1M} = rY_{1M}$, is calculated. The small parameter f^{in} is found together with f^{ex} from a common description of the observed energies of the isoscalar giant monopole and quadrupole resonances. The values of these parameters, calculated for ^{208}Pb, are found to be the following: $f^{ex} = -2.926$ and $f^{in} = 0.0875$. The Landau–Migdal parameter f' obtained from a fit to single-quasiparticle spectra via the symmetry potential $v(r)$ of Eq. (22) determines also the energies of the isovector spinless giant resonances. It was found that, within the considered model, the IVGDR energy is underestimated without taking the momentum-dependent forces into account. Apart from the IVGDR energy shift, the intensity of these forces, k'_1, determines also the excess of the integrated $E1$ photoabsorption cross section $\sigma^{\rm int}_{E1}$ over the Thomas–Reiche–Kuhn sum rule $\sigma_{\rm TRK} = 15A$ MeV mb : $\sigma^{\rm int}_{E1} = (1+k'_1)\sigma_{\rm TRK}$. Thus, the parameter k'_1 can be deduced from consistent description of the photoabsorption cross section in the vicinity of the IVGDR. It means that the DSD $E1$-reaction amplitudes of Eq. (15) can be evaluated within the model without the use of additional adjustable parameters. Since the experimental data concerned with the IVGQR energy are scanty, we deduce the parameter k'_2 by considering the DSD photoneutron and inverse reactions in the vicinity of the IVGQR. Such a procedure allows us to make within the model the predictions concerning the IVGQR main properties.

TABLE I. Values of adjusted mean-field parameters used in the calculations.

Nucleus	U_0 (MeV)	U_{ls} (MeV fm^2)	r_0 (fm)	a (fm)	f'
^{89}Y	55.210	31.885	1.21	0.613	1.052
^{140}Ce	55.815	32.095	1.21	0.625	0.975
^{208}Pb	56.39	33.354	1.21	0.63	0.976

One more input quantity for implementations of the PHDOM is the intensity of the imaginary part of the effective optical-model potential, $W(\omega)$. From a fit to the total widths of various giant resonances within the PHDOM "pole" version, it was found that $W(\omega)$ exhibits a saturation-like energy dependence [7,10]:

$$2W(\omega \geqslant \Delta) = \alpha\frac{(\omega-\Delta)^2}{1+(\omega-\Delta)^2/B^2}, \quad W(\omega \leqslant \Delta) = 0. \tag{23}$$

The "gap" parameter $\Delta = 3$ MeV and the "saturation" parameter $B = 7$ MeV are chosen as universal quantities, while the intensity parameter $\alpha \sim 0.1$ MeV^{-1} is further considered as an adjustable parameter, found within the PHDOM from a fit to the observed peak energy (or to an estimate of the total width) of a given giant resonance. As mentioned above, the real part of the optical-model addition to the mean field $P(\omega)$, appearing due to the spreading effect, is determined by $W(\omega)$ via a proper dispersive relationship [7,8,14]. The explicit expression for $P(\omega)$ obtained in Ref. [14] with the use of the parametrization given by Eq. (23) is rather cumbersome and not shown here.

In the concluding this section, we estimate the accuracy of the approximate expression (17) for the energy-averaged free p-h propagator (Sec. II B). Actually, this expression is obtained in Refs. [7,8] with the use of an approximate spectral expansion of the optical-model Green functions. The accuracy of this approximation can be verified by evaluation of the isoscalar monopole strength function $S^{(+)}_{V_0}(\omega)$, associated with the spurious external field $V_0 = 1$. For ^{208}Pb, we find that the calculated integral spurious strength $\int S^{(+)}_{V_0}(\omega)d\omega$ is quite small: of order 10^{-3}.

III. ENERGY-AVERAGED CROSS SECTIONS

A. Expressions for cross sections

The energy-averaged cross sections of photonuclear reactions considered below are expressed in terms of the energy-averaged strength functions and DSD-reaction amplitudes of Eqs. (14)–(16). In particular, the total cross section of the $(E1 + E2)$-photoabsorption is determined by the corresponding energy-weighted strength functions:

$$\sigma_{a,E1}(\omega) + \sigma_{a,E2}(\omega) = \frac{16\pi^3}{3}\frac{e^2}{\hbar c}\omega\left[S_1^{(-)}(\omega) + \frac{1}{20}\left(\frac{\omega}{\hbar c}\right)^2 S_2^{(-)}(\omega)\right]. \quad (24)$$

Here, ω is the photon energy. The strength functions $S_2^{(\pm)}(\omega)$ are of particular interest because they determine, among other things, the energies of the isoscalar and isovector giant quadrupole resonances. The photoabsorption cross section integrated over a given energy interval δ, $\sigma^{\rm int}(\delta)$ is also related to observable quantities.

Neglecting the fluctuating part the expression for the energy-averaged partial differential cross section of the DSD photoneutron reaction, accompanied by excitation of the IVGDR and IVGQR in the (Z,N) target nucleus and leading to population of the one-hole state μ^{-1} of the $(Z,N-1)$ product nucleus, can be presented as an expansion in terms of the first five Legendre polynomials:

$$\frac{d\sigma_\mu(\omega,\theta)}{d\Omega_n} = \sum_{\mathcal{L}LL'} B^{(\mathcal{L})n}_{\mu,LL'} P_{\mathcal{L}}(\cos\theta). \quad (25)$$

The expansion coefficients, expressed in terms of known kinematical factors and the photoneutron DSD-reaction amplitudes of Eqs. (15) and (16), can be written in the following form (in the following, the isobaric index n may be omitted for brevity):

$$B^{(\mathcal{L})}_{\mu,LL'} = 4\pi^{5/2} c_L c^*_{L'} \frac{e^2}{\hbar c}\omega \sum_{(\lambda)(\lambda')} i^{l'-l}(-1)^{j'+j_\mu} \times\left(\frac{\omega}{\hbar c}\right)^{L+L'-2} (L-1L'1|\mathcal{L}0) W(jj,'LL';\mathcal{L}j_\mu) \times\langle(\lambda)||Y_{\mathcal{L}}||(\lambda')\rangle M_{L,c} M^*_{L',c'}. \quad (26)$$

Here, $c_L = i^L[2L+1/(2L+1)!!]\sqrt{(L+1)/L}$, and $(L-1L'1|\mathcal{L}0)$ and $W(jj'LL';\mathcal{L}j_\mu)$ are the Clebsch–Gordan and Racah coefficients, respectively. In the IVGDR energy region, the expressions (25) and (26) are simplified ($L = L' = 1$) and can be presented as follows:

$$\frac{d\sigma_{\mu,E1}(\omega,\theta)}{d\Omega} = \frac{1}{4\pi}\sigma_{\mu,E1}(\omega)[1 + a_{2,\mu}(\omega)P_2(\cos\theta)]. \quad (27)$$

Here,

$$\sigma_{\mu,E1}(\omega) = \frac{16\pi^3}{3}\frac{e^2}{\hbar c}\omega\sum_{(\lambda)}|M_{1,c}(\omega)|^2$$

is the total cross section of the respective partial DSD (γ,n) reaction, and $a_{2,\mu}(\omega)$ is the anisotropy parameter:

$$a_{2,\mu}(\omega) = -\sqrt{6\pi}\sum_{(\lambda),(\lambda')} i^{l-l'}(-1)^{j+j'} W(2j'1j_\mu;j1) \times\langle(\lambda)||Y_2||(\lambda')\rangle M_{1,c}(\omega)M^*_{1,c'}(\omega)\Big/\sum_{(\lambda)}|M_{1,c}|^2. \quad (28)$$

The cross section $\sigma_{\mu,E1}(\omega)$ determines the partial probability $b_{\mu,E1}(\delta)$ for direct neutron decay of the IVGDR with the population of μ^{-1} single-hole state of the product-nucleus in accordance with the relation [7,10,17]

$$b_{\mu,E1}(\delta) = \int_\delta \omega^{-1}\sigma_{\mu,E1}(\omega)d\omega\Big/\int_\delta \omega^{-1}\sigma_{a,E1}(\omega)d\omega. \quad (29)$$

In Eq. (29), δ is the considered excitation-energy interval. In the absence of the spreading effect (that is, within the cRPA), the total probability of IVGDR direct neutron decay $b_{E1}(\delta) = \sum_\mu b_{\mu,E1}(\delta)$ is close to unity, as follows from Eq. (3). We neglect here a small contribution of IVGDR direct proton decay in the total probability. The spreading effect reduces substantially the quantity b_{E1}, so that the difference $1 - b_{E1}$ is the probability of IVGDR statistical (mainly neutron) decay, provided that the pre-equilibrium decay is neglected.

In accordance with the detailed-balance principle, the partial cross section for the DSD $E1 + E2$ neutron radiative capture by the neutron-closed-shell nucleus (Z,N), leading to population of the μ single-particle configuration of the product nucleus $(Z,N+1)$, $d\sigma^{inv}_\mu/d\Omega_\gamma$ is determined by the

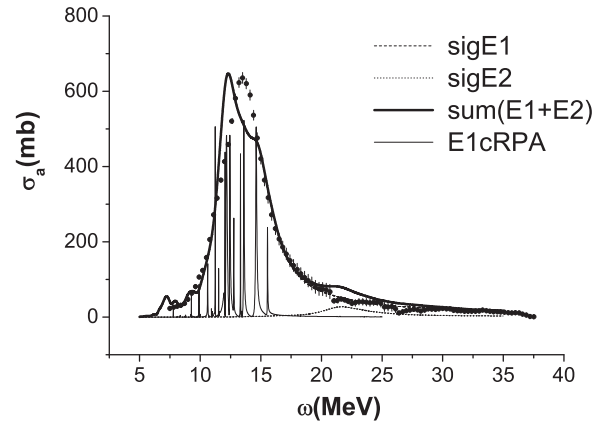

FIG. 1. Calculated total $E1 + E2$ photoabsorption cross section for ^{208}Pb in comparison with the experimental data of Ref. [18].

TABLE II. Values of the adjustable parameters determining the particle-hole interaction and the imaginary part of the effective optical-model potential.

Nucleus	k_1'	α (MeV^{-1})
^{89}Y	0.15	0.125
^{140}Ce	0.13	0.10
^{208}Pb	0.17	0.08

corresponding partial DSD (γ,n)-reaction cross section:

$$\frac{d\sigma_\mu^{inv}(\varepsilon)}{d\Omega_\gamma} = \frac{\omega^2}{2mc^2\varepsilon}\frac{d\sigma_\mu(\omega)}{d\Omega_n}, \tag{30}$$

with ε being the neutron kinetic energy and $\omega = \varepsilon - \varepsilon_\mu$. In accordance with the kinematics of the (n,γ) reaction considered, the DSD (γ,n)-reaction cross section in Eq. (30) is multiplied by the factor $(2j_\mu + 1)$. Therefore, this cross section should be evaluated with the use of Eqs. (15) and (16), where the factor n_μ equals unity as it takes place for the fully occupied neutron levels.

B. Reactions accompanied by excitation of IVGDR

We start the presentation of the calculation results obtained within the PHDOM with a description of photoabsorption by the ^{208}Pb target nucleus. Using Eqs. (10)–(14), (17)–(19), (23), and (24), we calculate the cross section of $E1$ photoabsorption by this nucleus and compare the results with the corresponding experimental data of Ref. [18] (see Fig. 1.) This comparison allows us to determine the adjustable parameters α and k_1', given in Table II. The integrated photoabsorption cross section calculated for the energy interval $\delta = 7.5$ to 37.5 MeV is 3633 mbn MeV, which is rather close to the corresponding experimental value of 3584 mbn MeV [18,19]. This point together with the satisfactory description of the IVGDR peak energy is an evidence for the consistency of the model. Also the calculated value of $\sigma_{E1}^{\rm int}$ is found to be close to the sum rule $\sigma_{\rm TRK}(1 + k_1')$. We note that the integrated cross section, calculated within the cRPA (3673 mbn MeV; see Fig. 1), slightly exceeds the corresponding value of 3633 mbn MeV obtained within the PHDOM, due to the inclusion of the spreading effect in the PHDOM. Similar results obtained for the ^{140}Ce and ^{89}Y target nuclei are presented in Table II and Fig. 2. The calculated $E1 + E2$ photoabsorption cross sections are also shown in Figs. 1 and 2 to demonstrate the small relative contribution of $E2$ photoabsorption to the total cross section. In the case of photoabsorption by ^{208}Pb, the ratio of $\sigma_{E2}^{\rm int}/\sigma_{E1}^{\rm int}$ calculated for the above-mentioned energy interval δ is found to be about 5%. To illustrate the contribution of Landau damping to the formation of the IVGDR total width (generally speaking, to the cross-section-shape line), we show in Figs. 1 and 2 the photoabsorption cross sections calculated within the cRPA (multiplied by the factor 10^{-1}). As follows from these figures, due to Landau damping the IVGDR cannot be considered as a single-level resonance.

The description of the DSD photoneutron and inverse reactions accompanied by IVGDR excitation is based on

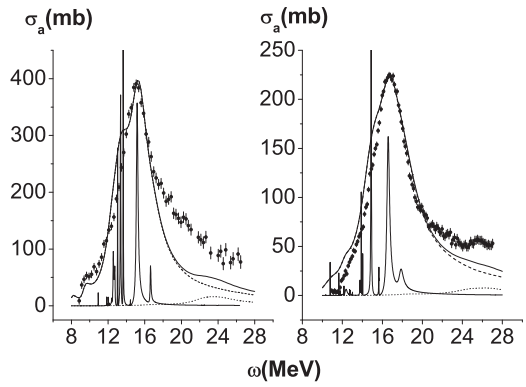

FIG. 2. Calculated total photoabsorption cross section for (left-side panel) ^{140}Ce and (right-side panel) ^{89}Y in comparison with the experimental data of Ref. [19]. The notations are the same as in Fig. 1.

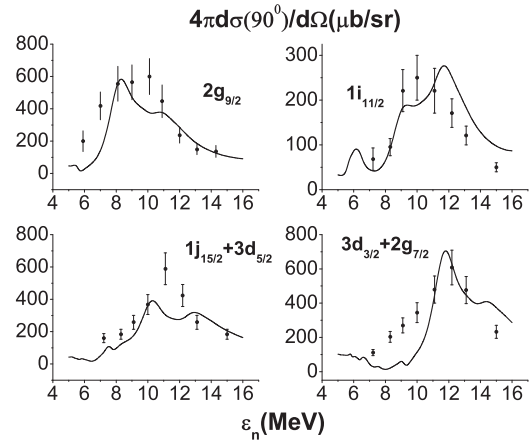

FIG. 3. Calculated partial differential ^{208}Pb(n,γ)-reaction cross sections in comparison with the experimental data of Ref. [20].

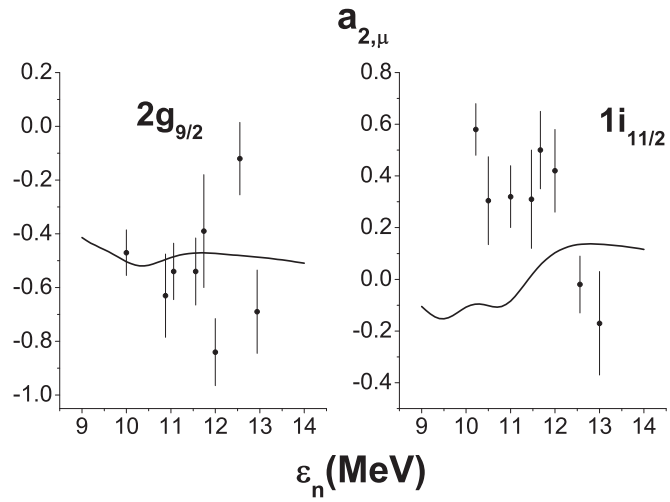

FIG. 4. Calculated anisotropy parameters for some partial differential ^{208}Pb(n,γ)-reaction cross sections in comparison with the experimental data of Ref. [20].

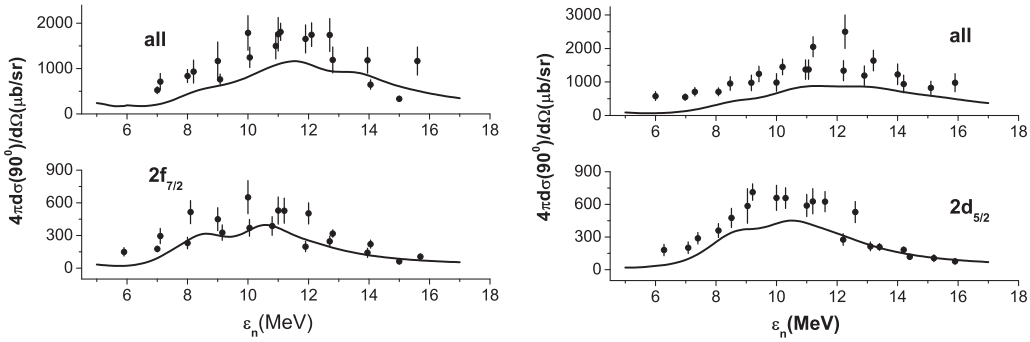

FIG. 5. Calculated (n,γ)-reaction partial cross sections for (left-side panel) ^{140}Ce and (right-side panel) ^{89}Y in comparison with the experimental data of Ref. [21].

Eqs. (27)–(30), in which the energy-averaged $E1$-reaction amplitudes are determined by Eq. (15). In such a description there are no new adjustable parameters (as compared with those used in the description of $E1$ photoabsorption). The energy-averaged partial differential ^{208}Pb(n,γ)-reaction cross sections (at 90°) calculated within the model and multiplied by the spectroscopic factor S_μ of the respective single-neutron state of the product nucleus are given in Fig. 3, in comparison with the corresponding experimental data of Ref. [20]. The S_μ values are taken from Ref. [5]. The anisotropy parameters $a_{2,\mu}$ calculated for two of the above-considered partial cross sections are shown in Fig. 4, in comparison with the corresponding experimental data of Ref. [20]. The calculated partial differential cross sections of neutron radiative capture by the neutron-closed-shell ^{140}Ce and ^{89}Y target nuclei are shown in Fig. 5, in comparison with the corresponding experimental data of Ref. [21]. Bearing in mind that the above-shown DSD-reaction cross sections are evaluated within the model without the use of free parameters, the description of the corresponding experimental data seems to be satisfactory.

Following Refs. [13,17], we evaluate the differential cross sections of the partial ^{208}Pb(γ,n) reactions, considering the results as the predictions of the model. The spectroscopic factors S_μ of neutron-hole states populated in this reaction are taken from Ref. [22]. The differential partial cross sections (at 90°) are shown in Fig. 6. Using the calculated partial cross sections $\sigma_{\mu,E1}(\omega)$ in Eq. (29) we evaluate the partial

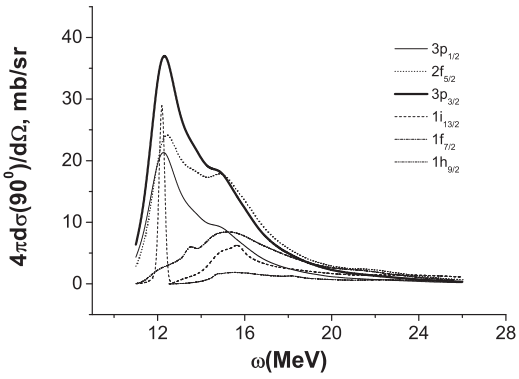

FIG. 6. Calculated partial differential (γ,n)-reaction cross sections for ^{208}Pb.

branching ratios for IVGDR direct neutron decay from the excitation-energy interval $\delta = 7.5$ to 37.5 MeV. The results are listed in Table III. The total probability for direct decay to the states listed in Table III is not large (about 13%). It means that the main contributions to the formation of this relatively-low-energy giant resonance are due to Landau damping and the spreading effect.

C. Reactions accompanied by excitation of IVGQR

Experimental information on the properties of the IVGQR is rather scanty (see, e.g., Ref. [3]). The common studies based on the use of the ordinary photonuclear reactions met with difficulties caused by a large IVGDR "tail" in the IVGQR region. This difficulty can be bypassed provided that specific subjects for study are chosen. Such a subject is the asymmetry (with respect to 90°) of the differential DSD (γ,n)- or inverse-reaction cross sections. As follows from Eqs. (25), (26), and (30), the asymmetry value is proportional to the product of the $E1$- and $E2$-reaction amplitudes of Eqs. (15) and (16), respectively, and, therefore, exhibits a nonregular energy behavior in the IVGQR region.

Usually, the asymmetry of the angular distribution of the partial (γ,n) reaction, leading to population of a neutron-hole state μ^{-1} of the product nucleus, is described by the quantity $\alpha_\mu(\omega,\theta_1)$ defined as follows [6]:

$$\alpha_\mu(\omega,\theta_1) = \frac{d\sigma_\mu^{(-)}}{d\Omega}(\omega,\theta_1) \Big/ \frac{d\sigma_\mu^{(+)}}{d\Omega}(\omega,\theta_1),$$

$$\frac{d\sigma_\mu^{(\pm)}}{d\Omega}(\omega,\theta_1) = \frac{d\sigma_\mu}{d\Omega}(\omega,\theta_1) \pm \frac{d\sigma_\mu}{d\Omega}(\omega,\pi-\theta_1), \quad (31)$$

with $\theta_1 = 55°$. The choice of this angle is motivated by the fact that $P_{L=2}(\theta_1) = P_{L=2}(\pi-\theta_1) \approx 0$. If the asymmetry is studied with the use of the reactions leading to population of several single-hole states lying within the excitation energy interval ΔE_x of the product nucleus, then the asymmetry is

TABLE III. Partial branching ratios for direct neutron decay of the IVGDR in ^{208}Pb.

μ	$3p_{1/2}$	$2f_{5/2}$	$3p_{3/2}$	$1i_{13/2}$	$1h_{9/2}$	$1f_{7/2}$
$b^n_{\mu,E1}(\delta)(\%)$	1.79	3.61	3.10	1.37	2.15	0.53

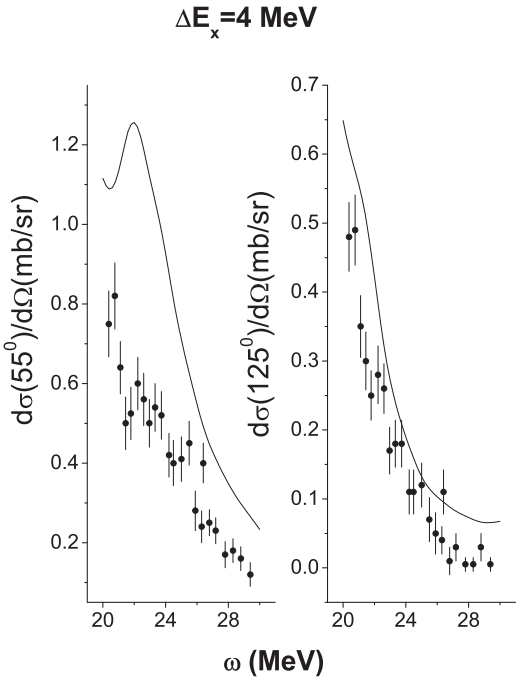

FIG. 7. Calculated differential ^{208}Pb(γ,n)-reaction cross sections in comparison with the experimental data of Ref. [6].

described by the quantity

$$\alpha(\omega,\theta_1) = \sum_\mu \frac{d\sigma_\mu^{(-)}}{d\Omega}(\omega,\theta_1) \Big/ \sum_\mu \frac{d\sigma_\mu^{(+)}}{d\Omega}(\omega,\theta_1), \qquad (32)$$

where summation is performed over the above-mentioned states.

Using the suggested model for the description of the photonuclear reactions that include excitation of the IVGQR, it is necessary to introduce the additional adjustable parameter k_2' (Sec. II). To better describe the asymmetry of the DSD differential photoneutron and inverse-reaction cross sections for target nuclei around $A = 208$, we take $k_2' = 0.1$. The calculated differential ^{208}Pb(γ,n_μ)-reaction cross sections (at θ_1 and $\pi - \theta_1$) for the case of $\Delta E_x = 4$ MeV and the

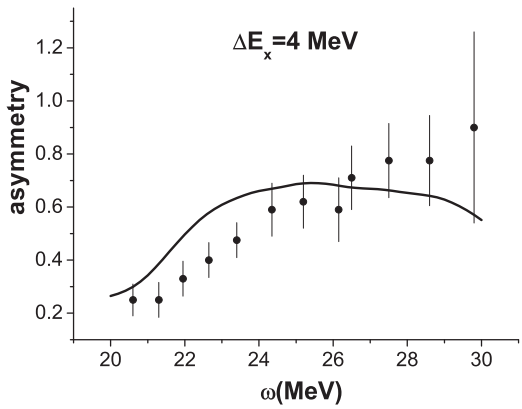

FIG. 8. Calculated asymmetry of the ^{208}Pb(γ,n)-reaction cross sections in comparison with the experimental data of Ref. [6].

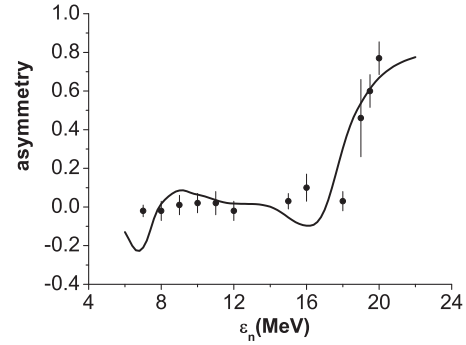

FIG. 9. Calculated asymmetry of the partial ^{208}Pb(n,γ_0)-reaction cross section in comparison with the experimental data of Ref. [23].

asymmetry quantity of Eq. (32) are shown in Figs. 7 and 8, respectively, together with the corresponding experimental data of Ref. [6]. The calculated cross section $d\sigma(\omega,55^\circ)/d\Omega_n$ is somewhat overestimated (Fig. 7) and leads to a rather poor description of the asymmetry quantity (Fig. 8). The reasons for these discrepancies are not clear now and will be studied in the future.

The asymmetry of the differential partial (n,γ_μ)-reaction cross section is described by the quantity $\alpha_\mu(\epsilon,\theta_1)$ defined similarly to Eq. (31) with $\varepsilon = \omega + \varepsilon_\mu$ being the captured-neutron kinetic energy. Calculated within the model the asymmetry quantities for the partial ^{208}Pb(n,γ_0)- and ^{209}Bi(n,γ_μ)-reaction cross sections describe satisfactorily the corresponding experimental data of Refs. [23] and [24], as it follows from Figs. 9 and 10, respectively.

The main properties of the IVGQR can be described within the model without the use of free parameters. As an example, we show in Fig. 11 the calculated strength function $S_2^{(-)}(\omega)$ together with that obtained within the cRPA and multiplied by the factor 0.2 for the ^{208}Pb nucleus. The calculated peak energy of 21.8 MeV and total width of 4.4 MeV are in agreement with corresponding data of Refs. [3,6]. The first moment of the strength function $\int_{(\delta)} \omega S_2^{(-)}(\omega) d\omega$ calculated for the large energy interval $\delta = 7.5$ to 37.5 MeV is found to

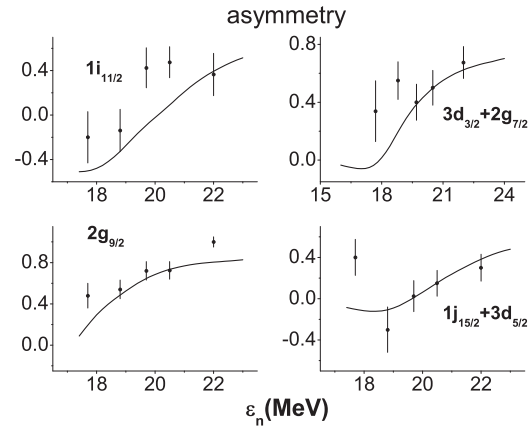

FIG. 10. Calculated asymmetry of the partial ^{209}Bi(n,γ)-reaction cross sections in comparison with the experimental data of Ref. [24].

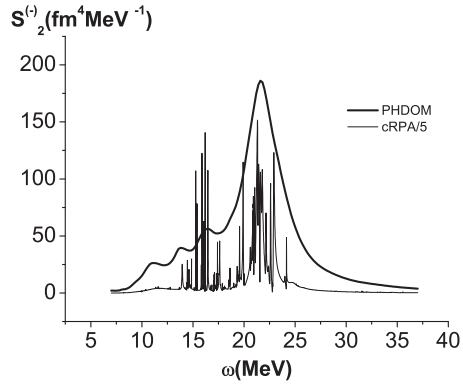

FIG. 11. Calculated strength function of the IVGQR in ^{208}Pb.

be in a good agreement with the energy-weighted sum rule $(\mathrm{SR})_2^{(-)} = \frac{5}{16\pi}\frac{\hbar^2 A}{m}\overline{r^2}(1 + 0.6k_2')$.

IV. CONCLUDING REMARKS

As a conclusion, one may say that the presented work is an example of a detailed application of the recently developed particle-hole dispersive optical model to the description of the simplest photonuclear reactions accompanied by excitation of the isovector giant dipole and quadrupole resonances in a few neutron-closed-shell nuclei. Within this semimicroscopic model, which is "economical" in the use of the input data, we describe satisfactorily, as a rule, the corresponding experimental data and make some predictions. The unique feature of the model is its ability to describe the direct + semidirect reactions induced by an external single-particle field. Having applied to the photoneutron and inverse reactions accompanied by the excitation of the isovector giant dipole resonance, such a description is obtained without the use of additional adjustable parameters.

Further studies can be related to (i) inclusion of the description of new appropriate target nuclei, (ii) further developments of the model (for instance, taking nuclear pairing into account), (iii) increasing the number of applications of the model such as the description of the direct + semidirect photoproton and inverse reactions, the simplest electronuclear reactions, and properties of the pigmy and second isovector giant dipole resonances.

ACKNOWLEDGMENTS

The authors are grateful to S. Shlomo for reading the manuscript and many valuable remarks made during his stay at NRNU "MEPhI" and to E. Harrison for the help in preparing the manuscript. This work is partially supported by Russian Foundation for Basic Research under Grant No. 12-02-01303-a.

[1] A. B. Migdal, Zh. Eksp. Teor. Fiz. **15**, 81 (1945).
[2] G. R. Bishop and R. Wilson, in *Handbuch der Physik*, Bd. 42 (Springer, Berlin, 1957).
[3] M. N. Harakeh and A. van der Woude, *Giant Resonances: Fundamental High-Frequency Modes of Nuclear Excitations* (Oxford University Press, New York, 2001).
[4] G. E. Brown, Nucl. Phys. **57**, 339 (1964).
[5] A. Likar and T. Vidmar, Nucl. Phys. A **591**, 458 (1995); **637**, 365 (1998).
[6] T. Murakami, I. Halpern, D. W. Storm, P. T. Debevec, L. J. Morford, S. A. Wender, and D. H. Dowell, Phys. Rev. C **35**, 479 (1987).
[7] M. H. Urin, Phys. At. Nucl. **74**, 1189 (2011).
[8] M. H. Urin, Phys. Rev. C **87**, 044330 (2013).
[9] B. A. Tulupov and M. H. Urin, Phys. At. Nucl. **75**, 1041 (2012).
[10] M. H. Urin, Nucl. Phys. A **811**, 107 (2008).
[11] B. A. Tulupov and M. H. Urin, EPJ Web Conf. **38**, 17010 (2012).
[12] A. B. Migdal, *Theory of Finite Fermi Systems and Applications to Atomic Nuclei* (Nauka, Moscow, 1965; Interscience, New York, 1967).
[13] V. A. Rodin and M. H. Urin, Phys. Lett. B **480**, 45 (2000); Phys. Rev. C **66**, 064608 (2002).
[14] B. A. Tulupov and M. H. Urin, Phys. At. Nucl. **72**, 737 (2009).
[15] S. Yu. Igashov and M. H. Urin, Bull. Russ. Acad. Sci.: Phys. **70**, 863 (2006).
[16] G. V. Kolomiytsev, S. Yu. Igashov, and M. H. Urin, Phys. At. Nucl. **77**, 1105 (2014).
[17] M. L. Gorelik and M. H. Urin, Phys. At. Nucl. **69**, 219 (2006).
[18] A. Veyssiere, H. Beil, R. Bergère, P. Carlos, and A. Lepretre, Nucl. Phys. A **159**, 561 (1970).
[19] http://cdfe.sinp.msu.ru/exfor/index.php
[20] I. Bergqvist, D. M. Drake, and D. K. McDaniels, Nucl. Phys. A **191**, 641 (1972).
[21] I. Bergqvist, B. Palson, L. Nilsson, A. Lindholm, D. M. Drake, E. Arthur, D. K. Daniels, and P. Varghese, Nucl. Phys. A **295**, 256 (1978).
[22] S. Gales, G. M. Crawley, D. Weber, and B. Zwieglinski, Phys. Rev. C **18**, 2475 (1978).
[23] D. M. Drake, S. Joly, L. Nilsson, S. A. Wender, K. Aniol, I. Halpern, and D. Storm, Phys. Rev. Lett. **47**, 1581 (1981).
[24] A. Hakansson, J. Blomgren, A. Likar, A. Lindholm, L. Nilsson, N. Olsson, and R. Zorro, Nucl. Phys. A **512**, 399 (1990).